Diving deep into the hair fiber: Ultrastructural analysis by PeakForce Quantitative NanoMechanics (QNM) mapping

Zhang,Guojin*; Edouard, Farahdia; Chavan, Manasi

Croda Inc, USA

* Guojin Zhang, 777 Scudders Mill Rd, Plainsboro, New Jersey, NJ 08536, United States
T: (609) 212-2410, Guojin.zhang@croda.com

Abstract
This study utilized a Quantitative NanoMechanics (QNM) mapping technique to acquire high-resolution modulus and adhesion images and characterize ultrafine structures of the hair. Modulus data characterizes the elasticity of the hair surface, while adhesion data relates to the water affinity (hydrophilicity) of the hair surface. Investigation shows that the outermost layer of virgin hair surface exhibits a unique network structure in which soft, hydrophobic domains are held together by rigid hydrophilic boundaries. Hair damage processes such as mild bleaching remove the soft hydrophobic complex of the top layer of the hair surface by eroding the hydrophilic boundaries, while intense bleaching creates pores/voids in the rigid hydrophilic boundaries. This study also shows that UV irradiation does not remove the hydrophobic layers but disrupts the hydrophilic boundaries. It is believed that hydrophobic domains and hydrophilic boundaries correspond to regions where lipids and proteins are present, respectively. Simple conditioning treatment with commonly used quaternary ammonium compounds such as behentrimonium chloride is not able to restore the original network structures of hair surface but deposits a hydrophobic layer with a thickness ~3 nm on the surface, significantly softening hair.

Key words: Ultrafine structure, Quantitative NanoMechanics (QNM) mapping, damaged hair, hair repair.

Introduction

Human hair is considered as nanocomposite biofibers due to its complex hierarchical nanostructure, and the characterization of hair ultrafine structure is critical to improve our fundamental understanding of hair properties. The main tool used to characterize hair ultrastructure in early studies was Transmission Electron Microscopy (TEM) (1-3). One of disadvantages of TEM is that it requires ultra-thin samples, which is particularly difficult to prepare from the cuticle surface. Additionally, the sectioning and staining process required by this technique may disrupt the natural structure of the hair. The advent of Atomic Force Microscopy (AFM) technique offered researchers an alternative way to explore nanostructures of hair due to its high resolution and non-destructive nature. Research has demonstrated that AFM can characterize changes in internal ultrafine structures of hair by acquiring three-dimensional morphological images of cross-sections of virgin and damaged hair (4). Additionally, the development of various AFM technologies has allowed scientists to further study nano-tribological, nano-mechanical properties and local surface potentials of hair surface, which cannot be achieved through scanning electron microscopy (SEM) or TEM (5-9).

A variety of AFM techniques have been extensively used to investigate the surface properties of hair from various aspects. For instance, researchers have used the friction imaging and adhesion image to explore nano-tribological properties of the outer layer of hair surface and have studied the roles of fatty acids such as 18-methyl eicosanoic acid (18-MEA) in the structural integrity of the cuticle (10-12). The surface static charges that directly affects hair fizziness can also be characterized on the nanoscale though the surface potential mapping with Kelvin probe microscopy, gaining insight of charge build-up and dissipation on virgin, damaged and conditioner-treated hair (9).

The sensory properties of hair are largely influenced by the mechanical properties of hair surface, which are determined by the structure of the underlying fiber biological network and the sub-lamellar structure of the hair surface (13-14). Therefore, the nano-mechanical characterization of hair surface is of great interest in cosmetic science, not only helping to evaluate the impact of

cosmetic products on the hair surface, but also providing a better understanding of the various composite structural properties of the hair surface. Early measurements of the mechanical properties of hair surface were achieved by indentation, in which a hard tip of known size and geometry is pressed into the hair surface under a short influence of pressure, and a series of indentation load-displacement curves were acquired from which hardness and Young's modulus were calculated (15). The mechanical properties were really measured at the microscale and the indentation was invasive. The advent of AFM techniques enables users to control a significantly smaller indentation load, shallower indentation depth and effective contact volume. The combination offers us the unique opportunity to probe local mechanical property within small domains at nanoscale (5). However, measurements can only be made through force modulation or force-distance curves in various points of hair surface. One disadvantage of this measurement is that it is difficult to directly relate the mechanical properties to the nanostructure of the hair surface since two images cannot be acquired simultaneously.

With the introductions of pulsed-force mode to AFM operation and unique pre-calibrated PeakForce Tapping probes, PeakForce Quantitative NanoMechanics(QNM) mapping was developed. This technique enables researchers to simultaneously measure mechanical properties such as modulus, adhesion and energy dissipation when acquiring a topographic image, and quantitative data can help researchers discern materials that are seen in atomic resolution topographic images. In previous hair studies, this technique was used to measure the hardening of the keratin structure along the follicle axis while simultaneously quantifying the local keratin network architecture and disclose sequence of biological and structural events during hair keratinization (16). In this study, we utilized this technology to delve into ultrafine structural features of the hair surface and gain better understanding of damages caused by UV and bleaching. The impact of hair treatments such as conditioners on the ultrastructural features of damaged hair was assessed.

Materials and Methods

Studies were conducted on Caucasian dark brown and light blonde hair purchased from International Hair Importers & Products Inc. (Glendale, NY). Before analysis, all hair was washed with a basic Sodium Laureth Sulfate (SLES) and cocamidopropyl betaine (CAPB) shampoo and rinsed with deionized water.

HAIR BLEACHING PROCEDURE

Caucasian dark brown hair was bleached using a 1:2 ratio of a commercial bleach powder, Clairol Professional BW Powder Lightener (The Wella Corporation, Calabasas, CA) mixed with a 40-volume developer from Salon Care Professional (Arcadia Beauty Labs LLC, Reno, NV). The resulting mixture was applied to dry hair at a weight ratio of mixture: hair = 10:1. For a mild hair bleaching process, the bleaching time was controlled to 20 minutes; for a more aggressive bleaching experiment, hair was bleached for 30 minutes twice, for a total of 1 hour. This is referred to as “2x bleached hair”.

Right after bleaching, hair was shampooed twice, then soaked in deionized water for 2 hours, followed by a rinse with deionized water for 30 seconds, and then blow-dried with a hair dryer set on the warm setting. Hair samples were then placed in controlled humidity (~45% RH) for 24 hours before measurements were conducted.

UV DAMAGE OF HAIR

Caucasian light blonde hair was damaged via UV using a Ci 3000+ Xenon Weather-Ometer (Atlas, Mount Prospect, IL U.S.) equipped with a water-cooled xenon arc lamp positioned in the center of the chamber and a rotating sample rack at the periphery where aluminum panels are installed. ~100 hair fibers per sample were mounted on an aluminum panel. UV irradiation was set to 50W/M^2 with a wavelength range of 300-400 nm. The temperature and relative humidity of the chamber were controlled at 40°C and 65%, with a UV exposure time of 10 hours, which is equivalent to about 1.5 days of ultraviolet exposure in Philadelphia, Pennsylvania, USA, from

June to August. The UV damaged hair was then placed in controlled humidity (~45% RH) for 24 hours before measurement was conducted.

HAIR TREATMENT WITH CONDITIONERS

Mildly bleached hair, using the bleaching procedure described above, was treated with a 1% Behentrimonium Chloride (BTAC) conditioner formula using the following procedure: The conditioner was applied to wet hair at a weight ratio of 0.25 to dry hair, massaged into the hair for 30 seconds, then left on for 2 minutes. The hair was then rinsed with tap water for 30 seconds, followed by a final rinse with deionized water for 30 seconds, then dried with a blow dryer set on the warm setting. The conditioner treated hair was placed in controlled humidity (~45%) for 24 hours before measurement was conducted.

PEAKFORCE QUANTITATIVE NANOMECHANICAL MAPPING (QNM)

PeakForce QNM mapping was conducted using a DimensionIcon with ScanAsyst AFM with a Nanoscope VI controller and operated using Nanoscope controller V10.0 software (Bruker, Billerica, MA, USA). The nanomechanical property mapping is based on the individual force vs. the separation curves obtained from each tap, as displayed in Fig.1 (top left). The force curve is logged for each map pixel of the scanned image, which provides the mapping of all the investigated properties in a single scan line. The four data channels, namely height image, modulus image, adhesion image and energy dissipation image, were used in this study as shown in Fig.1 (bottom).

All images were captured in air at ~ 45% RH with the stiffer RTESPA-300 probe (Bruker, Billerica, MA, USA). Before the measurement, a probe calibration process was implemented following a workflow from the Nanoscope software. The calibration of the deflection sensitivity was conducted on the sapphire sample and the exact spring constant of the cantilever is determined

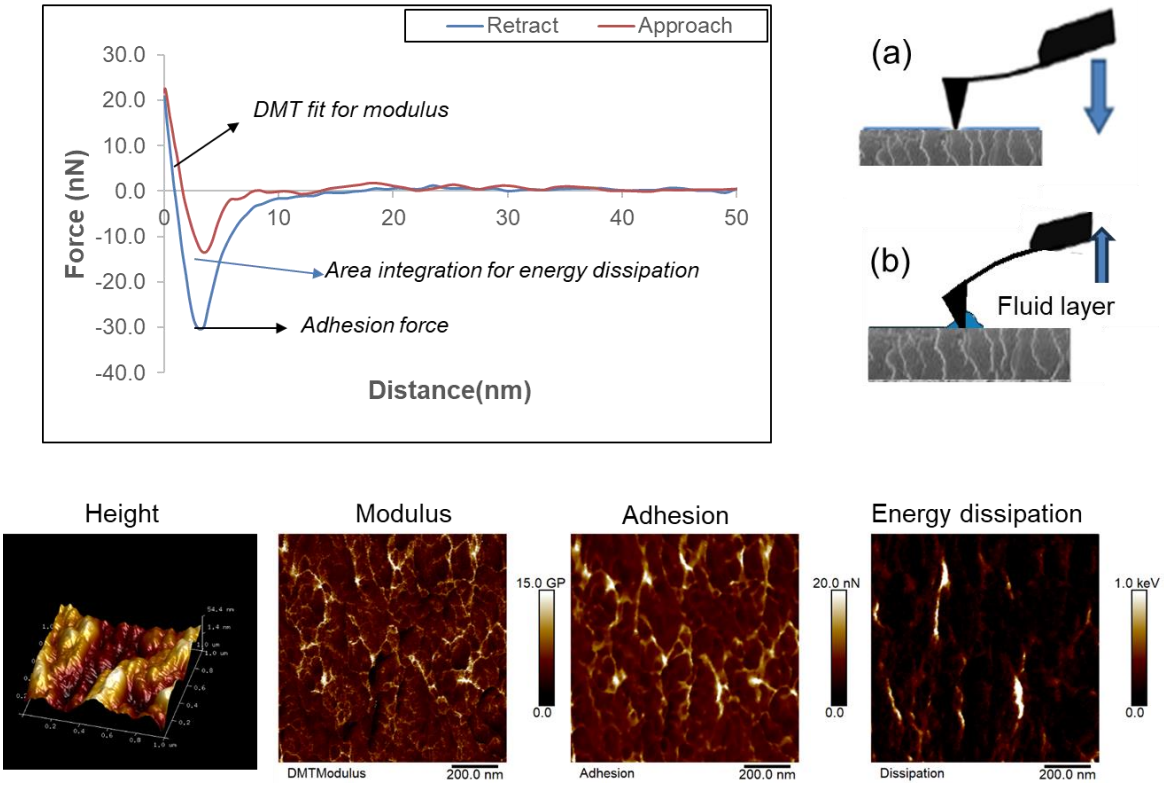

Figure 1. **Top left**: A single cycle force vs. separation curve obtained from a single tap of the AFM tip on hair surface. **Top right**: Schematic graphs showing (a) a AFM tip approaching hair surface where the cantilever deflects and (b) a AFM tip retracting from hair surface where adhesion force pulls the tip down. **Bottom**: Images of topography, Derjaguin Muller-Toporov (DMT) modulus, adhesion force, and energy dissipation that are simultaneously acquired from a hair surface by PeakForce-QNM.

by the Thermal Tune function. The tip radius is measured by a standard titanium sample using the Tip Qualification function on Nanoscope software. The Young's modulus was calculated by fitting part of the retracting curve using the Derjaguin–Muller–Toporov (DMT) model of elastic interaction with consideration of the adhesion force as marked in Fig. 1 (top left). The fitting region was set between 90% and 30% of the force range for the retract curve. The image was captured at 3 to 5 locations on each hair fiber and 7-10 hair fibers were examined for each sample, with 1 × 1 μm2 images being collected at each site.

(1) DMT modulus calculation

The Young's modulus E* was obtained by fitting the retract curve to the DMT model:

$$F - F_{adh} = \frac{4}{3} E^* \sqrt{R(d - d_0)^3}$$

Where F is the applied force, F_{adh} is the adhesion force between probe and the surface, R is the tip radius, $(d - d_0)$ is the sample deformation, E* is the elastic modulus.

Assuming modulus of the tip is infinite, the sample modulus to be calculated as follows:

$$E^* = \frac{E_s}{1 - \nu_s^2}$$

Where E_s is the sample modulus; ν_s is the sample Poisson ratio, which is a ratio of transverse contraction strain to longitudinal extension strain in the direction of the stretching force. The standard value of sample Poisson ratio used in this study is 0.3. The calculations of the modulus with the DMT model were taken in real time during the scan for every probe tap.

(2) Adhesion Force

The adhesion force was determined as the lowest point in the force vs. distance curves, as marked in Fig.1 (top). As the AFM tip scans a hair sample in air, moisture absorbed on the substrate forms a capillary meniscus at the point of contact between the tip and sample (shown in Fig.1 (top right)) and creates an adhesion force to the tip. It has been reported that adhesion depends on the thickness of the adsorbed water layer (17-18). Therefore, adhesion force determines the degree of hydrophobicity or hydrophilicity of hair surface.

(3) Statistical analysis

Statistical analysis was performed with the software package Minitab. Kruskal–Wallis ANOVA with multiple comparisons of mean ranks was used to assess the differences among the experimental groups. The significance level p value was set at 0.05.

Results

PeakForce QNM mapping was used to scan areas near the intercellular region, so called inner zones of the cuticle surface of virgin hair shown in Fig. 2 (top left). In these areas, the cuticle is subject to relatively minimal damage during daily grooming or care and may be most relevant to its original structure. A typical high-resolution height image, modulus image, and adhesion image are shown in Fig. 2. As depicted by the color bar, darker colors in the images represent lower values of height, modulus, or adhesion, while lighter colors represent higher values of height,

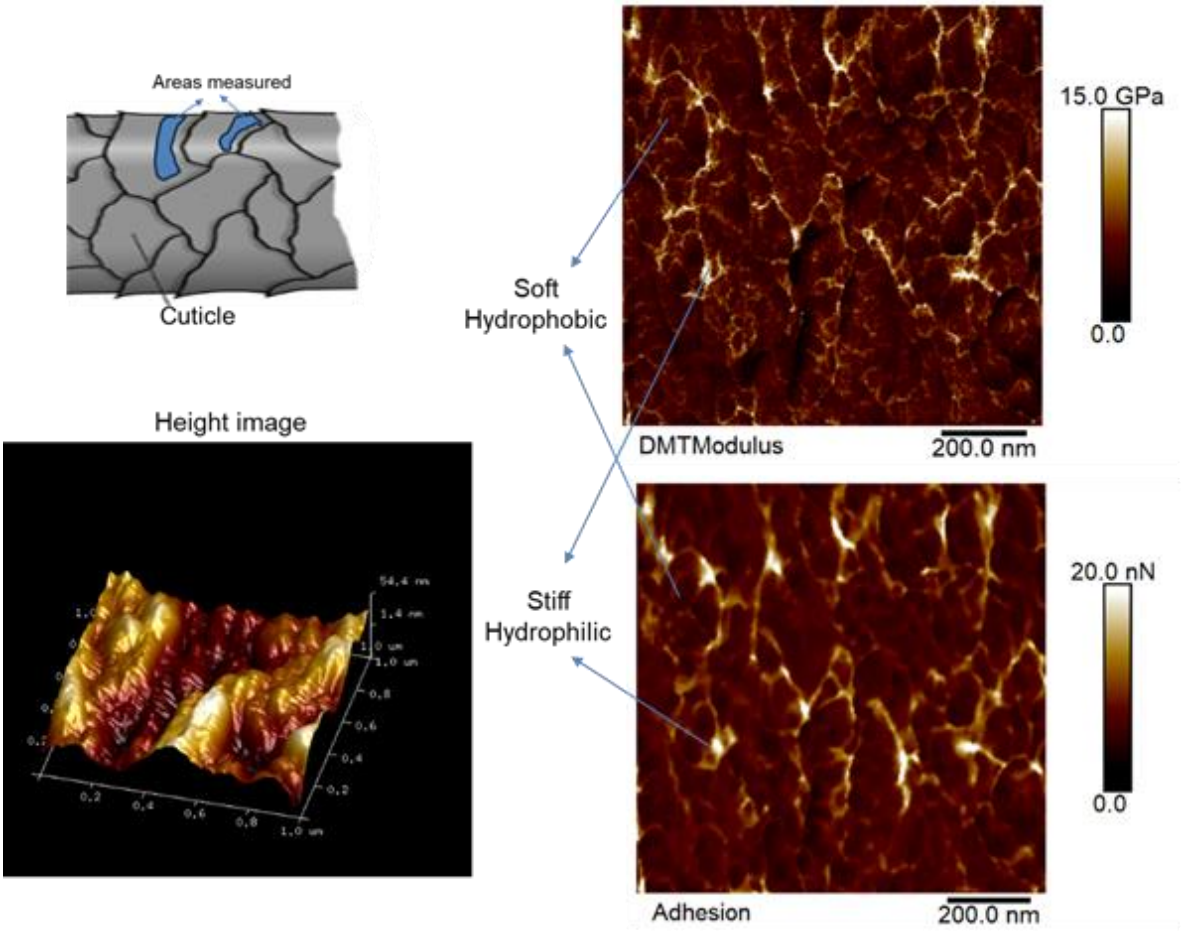

Figure 2. QNM images acquired from the inner surface of cuticle cell of cadark brown virgin hair. **Top left**: Schematic graph of the hair cuticle marked with areas where images were scanned. **Down left**: A height image of cuticle surface. **Top right**: A DMT modulus image of cuticle surface; **Down right**: A adhesion force image of cuticle surface.

modulus, or adhesion. The DMT modulus image shows that the modulus of hair surface varies significantly, with some areas less than 1 GPa and other regions as high as 20 GPa (Fig.2, top right). When analyzed in conjunction with the adhesion image (Fig. 2, down right), it is interesting note that areas with low modulus correspond to areas of lower adhesion, while areas with higher modulus correspond to areas of high adhesion. As the adhesion data correlates to water affinity of the hair surface, Fig. 2 shows that the cuticle surface of virgin hair exhibits a network-like structure in which dominated soft (with low modulus) hydrophobic domains (lower adhesion) are held together by rigid (with high modulus) hydrophilic boundaries (high adhesion). Two sets of images (height, modulus, and adhesion) acquired from the inner regions of two different hair fibers are displayed in Fig. 3. Although the size and shapes of hydrophobic domains vary with different hair fibers, cuticle surfaces share similar network-like structural features and are predominately covered with soft hydrophobic materials.

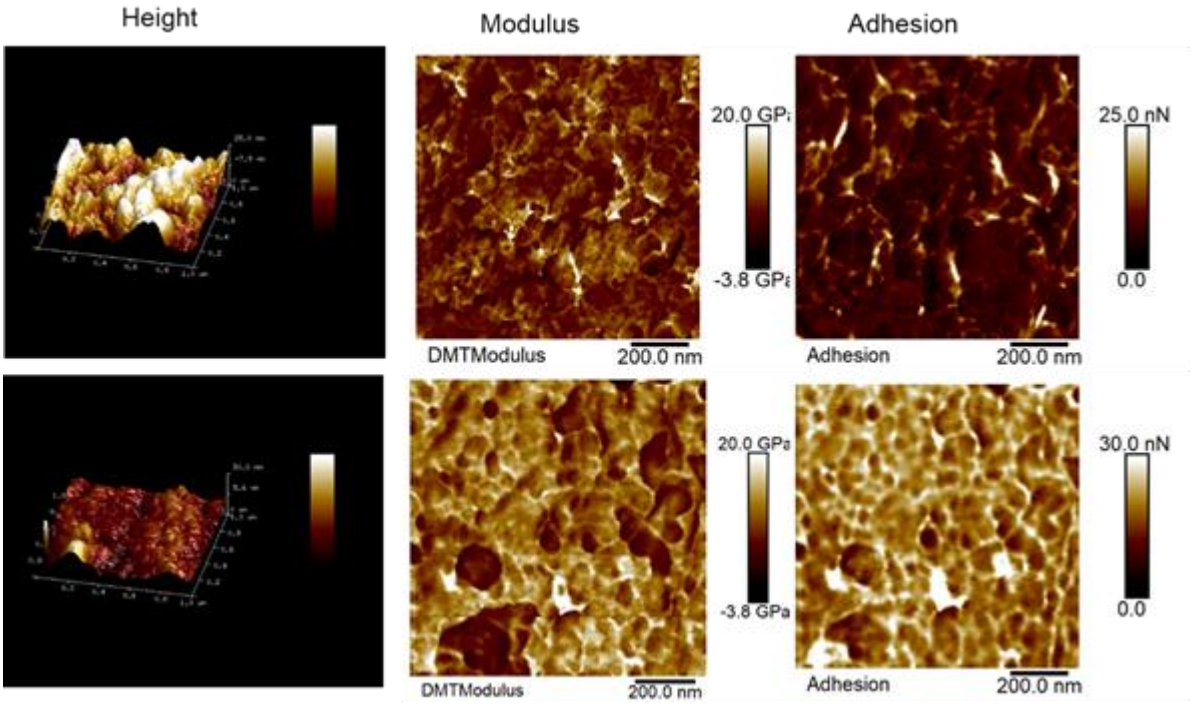

Figure 3. Height, modulus, and adhesion images acquired from the inner surface region of cuticle cell of two different virgin hair fibers.

Fig. 4 shows modulus and adhesion images scanned near the edge regions of cuticle cells. Although the surface structure still exhibits network-likes structures, the sizes of soft & hydrophobic domains are much smaller compared to the inner regions of the cuticle as shown in Fig. 2 and 3. Relatively high adhesion is observed where scratches and dents are present, indicating a higher affinity for water in these areas (Fig. 4, upper right). In some large areas close to the cuticle edge, high modulus and adhesion were observed (Fig. 4, bottom). This can be attributed to the fact that the cuticle edges are subject to abrasion, which can remove some of the soft hydrophobic material, resulting in exposure of the underlying rigid proteinaceous

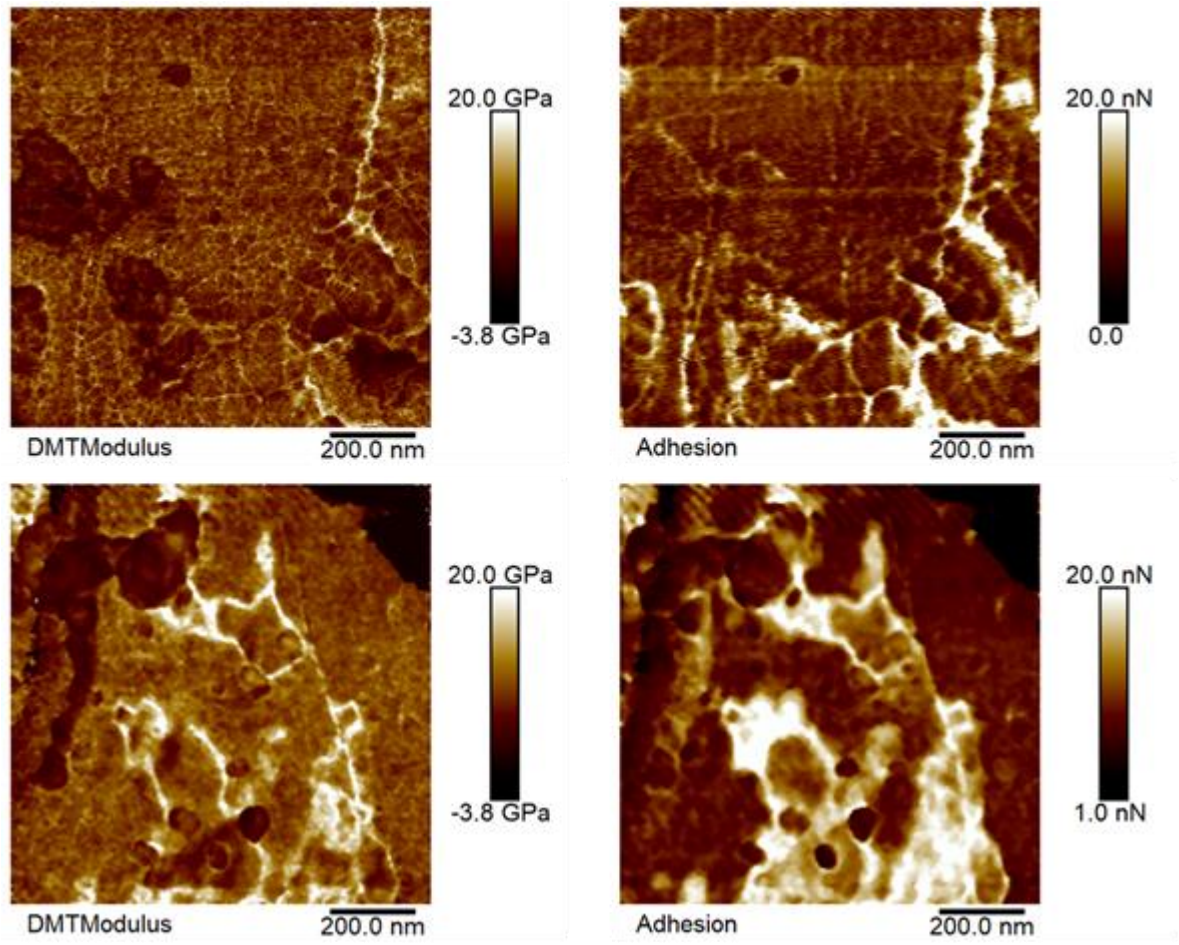

Figure 4. Typical DMT modulus and adhesion force images acquired in the middle to near edges of cuticle cells of virgin hair.

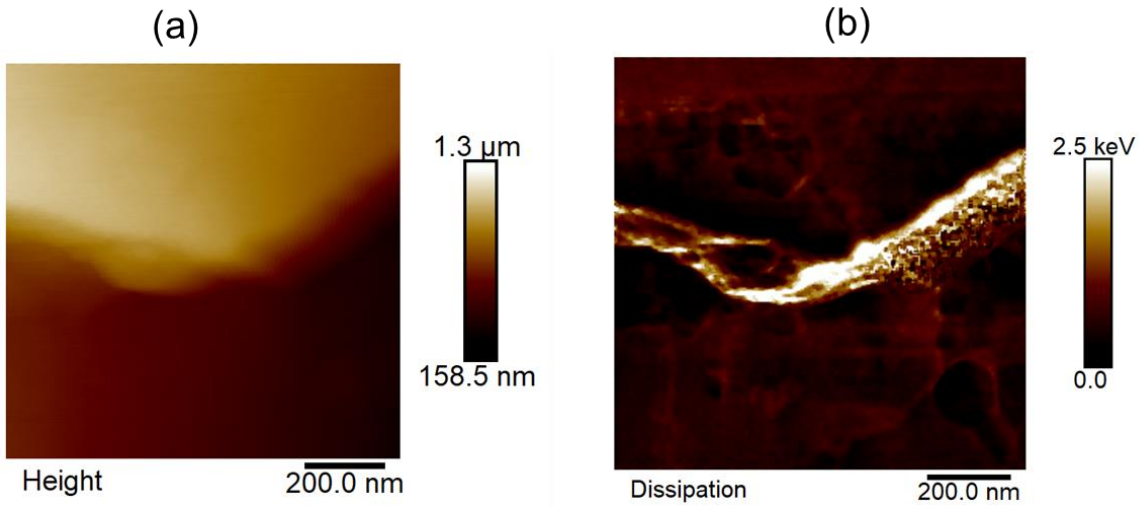

Figure 5. Height image (a) and energy dissipation image (b) of a cuticle edge.

material which tends to attract water molecules. The cuticle edge generally shows much higher energy dissipation than the surrounding areas (in Fig.5), which explains why the cuticle edge is more susceptible to damages from environmental insults.

To gain further understanding of the complex structure of the top layer of the hair surface, the hair was bleached or UV damaged. Both treatments are known to oxidize hair proteins, and bleaching is known to remove the hydrophobic layer whereas UV irradiation does not.

Fig. 6 shows comparisons of height images, DMT modulus images and adhesion images scanned from virgin (top row), mild bleached (middle row) and 2x bleached Caucasian dark brown hair (bottom row). Images were acquired near the inner regions of cuticle cells as shown in Fig.2 (top left) and the height images were presented in the same scale. It is noted that the roughness of the surfaces of bleached hair decreases, especially the surface of 2X bleached hair. When analyzed in conjunction with modulus and adhesion images, it has been found that bleaching removes the soft hydrophobic complex on the top layer of hair surface and significant modulus loss occurs in hydrophilic rigid boundaries, indicating that those areas are more susceptible to bleach erosion (see arrows). Aggressive bleaching (2x bleached hair) not only removes more of the hydrophobic layer of hair surface, but also creates many pores/voids

where significant modulus loss was observed. Comparisons of adhesion images revealed that the stronger the bleaching process, the greater the adhesion force and the larger the hydrophilic area.

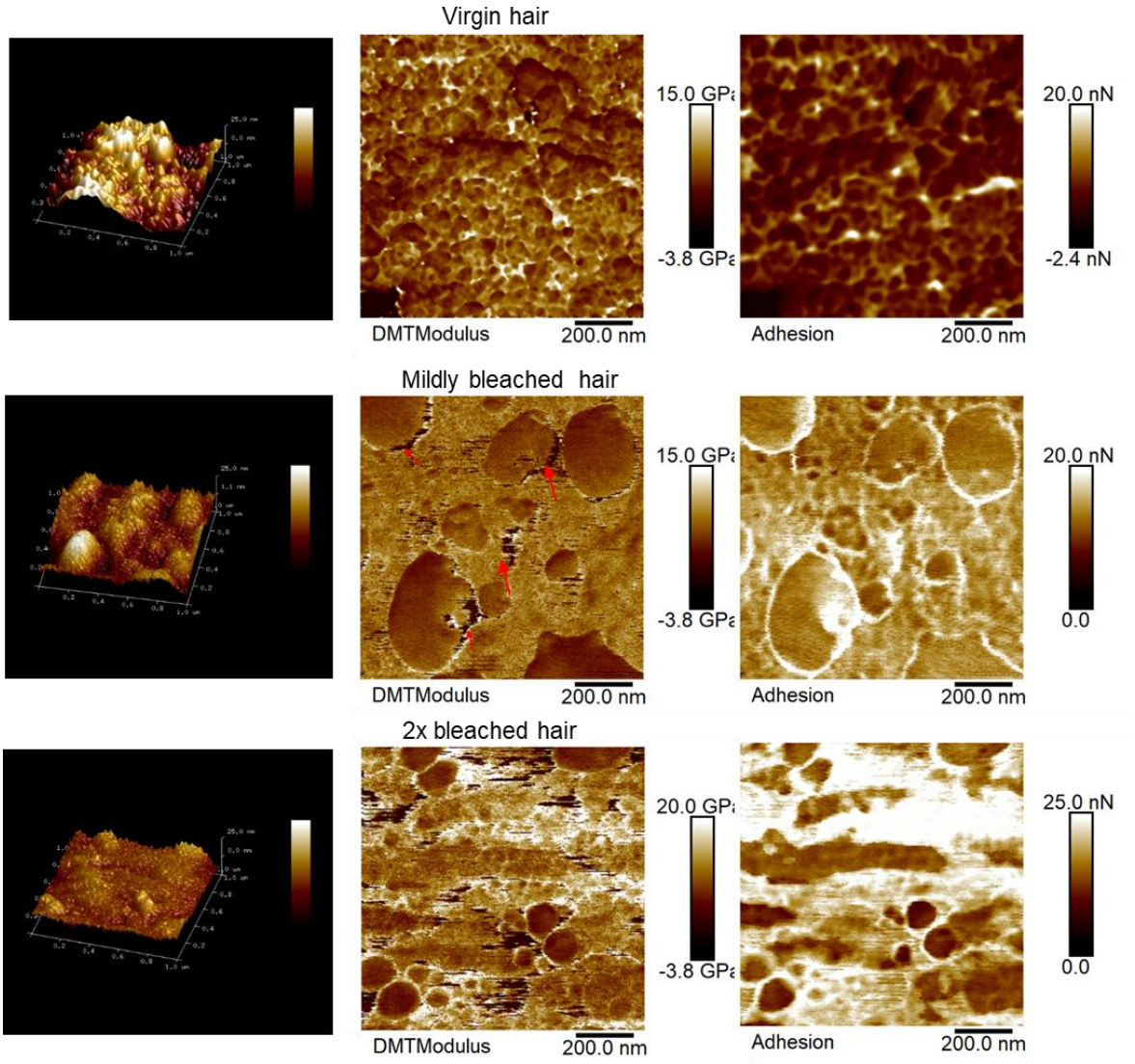

Figure 6. Comparison of height images, DMT modulus images and adhesion images acquired from virgin hair (top row), mildly bleached hair (middle row) and 2x bleached hair (bottom row). Images were acquired near the inner surface regions of cuticle cells.

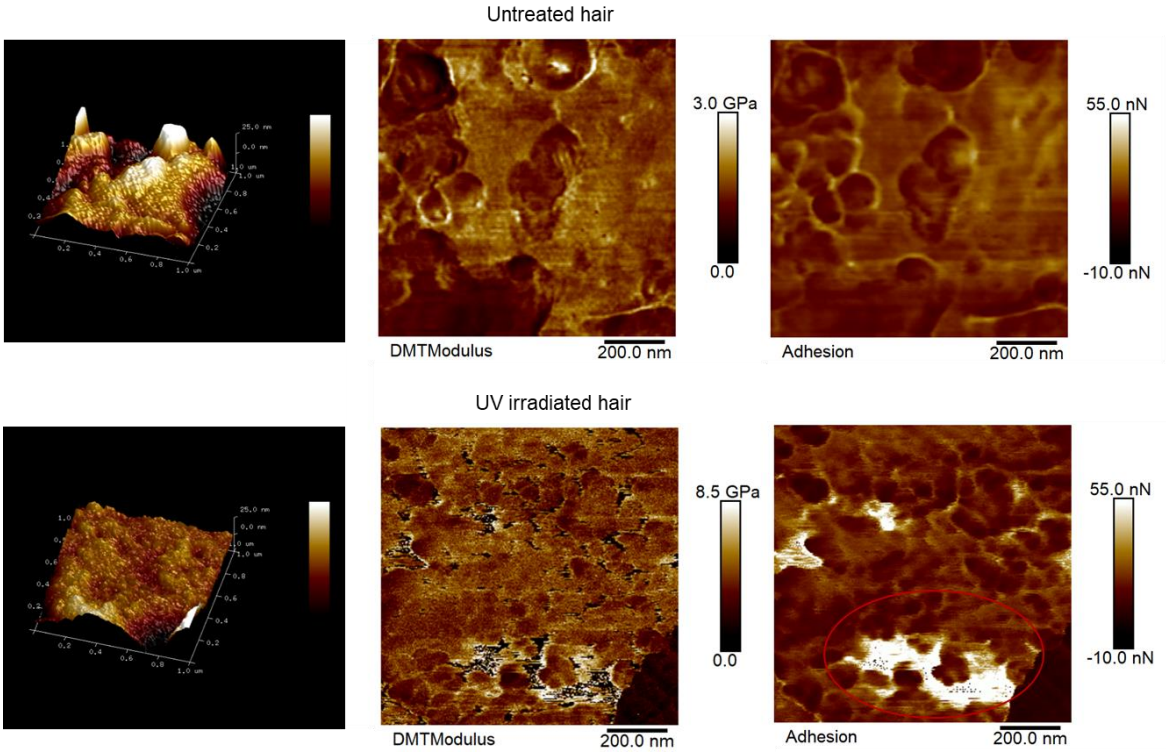

Figure 7. Comparison of height images, DMT modulus images and adhesion images acquired from untreated light blonde hair (top row), and UV irradiated hair (bottom row).

Figure 7 shows comparisons of height images, modulus images and adhesion images acquired from surfaces of Caucasian light blonde hair with and without UV irradiation. The soft hydrophobic domains are visible on the surfaces of both untreated and UV irradiated hair as shown in both modulus and adhesion images. However, by examining the modulus images of UV treated hair, it was observed that UV irradiation nearly destroyed the hydrophilic boundaries where massive pores/voids were created. Large areas with significantly high adhesion (see circled areas in the adhesion image) were frequently observed on the surface of UV-treated hair. This may be due to the damaged area absorbing multi-layers of water, or UV exposure causing different chemicals to form on the surface of the hair. More investigation is needed to clearly understand why.

The average modulus of the surface of UV-irradiated hair is much smaller than that of the bleached hair used in this experiment, while adhesion force exhibited an opposite trend, suggesting that both modulus and adhesion force may vary depending on the hair types and hair treatment/damage history. The size and shapes of hydrophobic domains changes with individual fibers. Within a single fiber, the modulus and adhesion values vary with difference zones of hair cuticle cells, with the inner regions being more hydrophobic and softer, and those closer to the cuticle edge being rigid and hydrophilic, as shown in Fig. 5.

To explore the effect of conditioner treatment on surface structure of hair, mild-bleached hair was treated with 1% behentrimonium chloride (BTAC). A comparison of height images displayed in Fig. 8 with the same scales (25nm) shows that the BTAC treatment reduces the surface roughness of mild-bleached hair. By averaging modulus and adhesion values from images that were acquired at more than 30 locations on 10 fibers per sample, comparisons of modulus and adhesion on surfaces of virgin hair, mild-bleached hair with and without BTAC treatment were made and results are displayed in Fig.9. Modulus data shows that mild bleaching does not significantly change the surface modulus of hair compared to virgin hair. but BTAC treatment significantly reduces modulus values and softens the hair surface compared to untreated bleached hair. As expected, mild bleaching increases adhesion force of hair surface compared to virgin hair and hair surface becomes more hydrophilic. The decreased adhesion value in BTAC treated hair has shown that BTAC treatment restores the hydrophobicity of the hair surface.

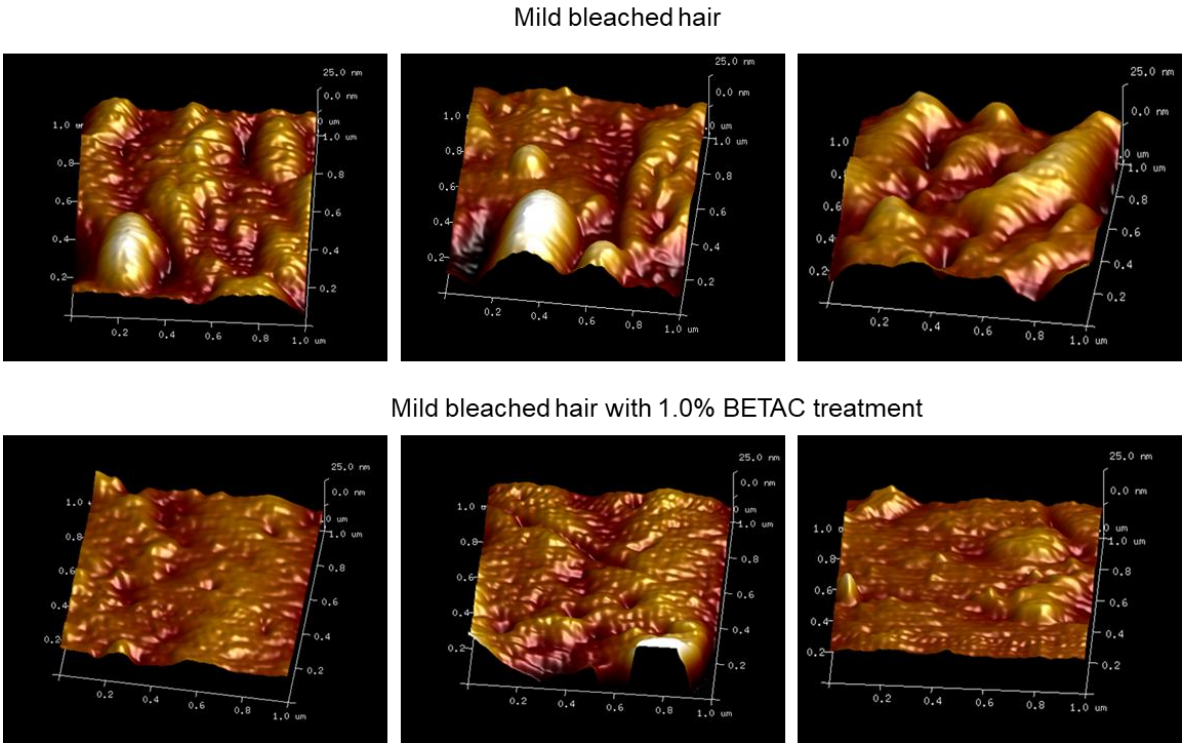

Figure 8. Morphological comparison of mild bleached hair before and after treatment. **Top row**: Height images scanned from the surfaces of different mild bleached hair fibers. **Bottom row**: Height images scanned from surfaces of 1% BTAC treated hair fibers.

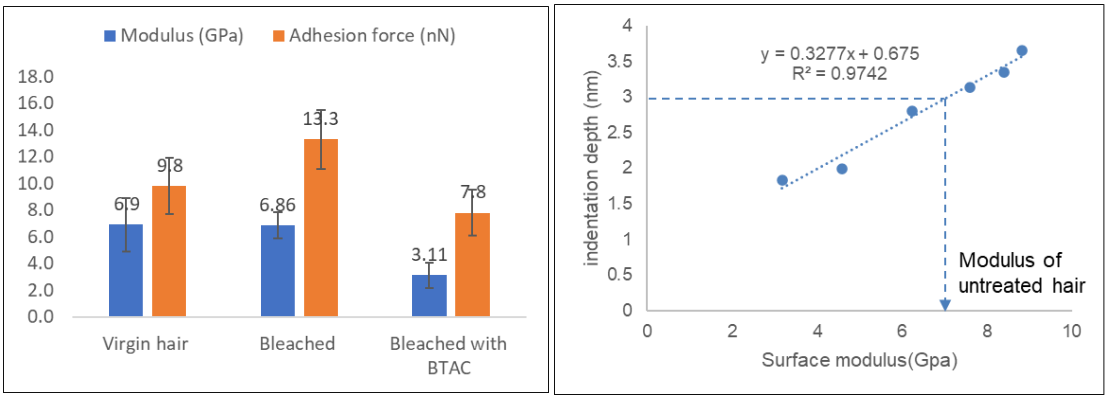

Figure 9. **Left**: Comparison of modulus an adhesion force of virgin hair, mild bleached hair with/without BTAC treatment. **Right**: The relationship of indentation depth vs surface modulus.

The thickness of BTAC on the hair surface was determined by measuring the relationship of modulus versus indentation depth (shown in Fig.9, right). This is achieved by increasing the load force on the AFM probe and indenting the AFM tip further into the hair surface until a point is reached where the hair modulus is equal to the modulus of untreated hair and the corresponding indentation depth is the BTAC thickness. The thickness of BTAC is estimated to be approximately 3 nm. By closely examining multiple modulus images of BTAC treated hair samples, it was found that although BTAC restored hydrophobicity of hair, it did not repair the voids/pores generated from bleaching, where significantly lower modulus is evident, as shown in the circled areas of Fig 10.

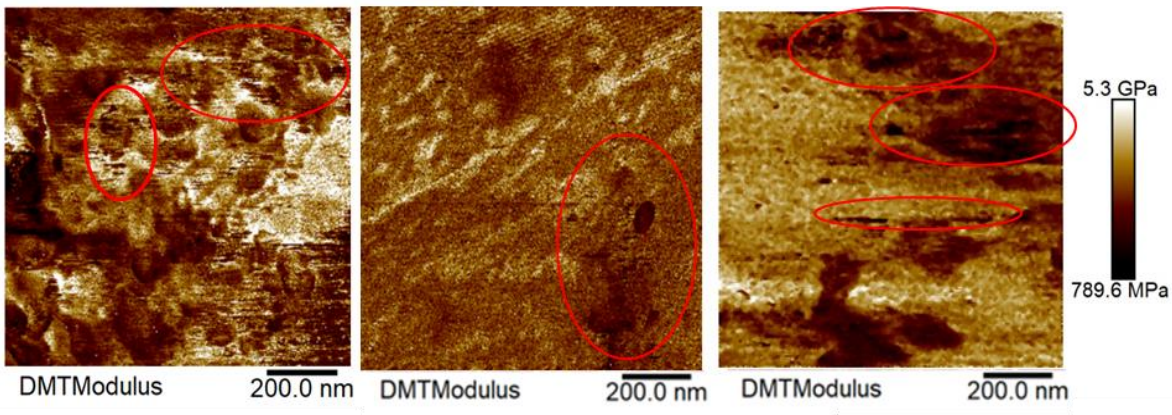

Figure 10. Modulus images obtained from BTAC treated hair.

Discussion

It is well known that cuticle cells have complex layered sub-structures and the outermost layer is called the outer β-layer. With the topographic image in conjunction with modulus and adhesion images, this study revealed that hair surface (most likely inferred to be the outer β-layer) is a network-like structure with larger soft hydrophobic domains surrounded by rigid hydrophilic boundaries. The outer β-layer is known rich of free and covalently bond fatty acid (e.g 18-methyleicosanoic acid) (19-20), therefore, it is believed that the soft hydrophobic domains observed in modulus and adhesion maps are dominated by lipid composition. The

significant modulus loss due to UV or bleaching treatments occurred in the hydrophilic boundary regions of the hair surface, and both UV irradiation and bleaching treatment are known to oxidize proteins by breaking disulfide bonds. It can be speculated that the rigid hydrophilic boundary may be composed mainly of proteins. This network composite structure helps maintain the integrity of the hair surface and minimizes the loss of surface structural lipids during daily grooming and care.

Conclusions

In this study, by analyzing modulus and adhesion images, a network-like structure where soft hydrophobic lipid domains are held together by rigid hydrophilic proteinaceous boundaries was discovered on the outermost layer of undamaged hair. Comparing the ultrastructure of virgin, bleached, and UV-damaged hair provides greater insights of how hair is damaged in different ultrastructural domains that correlates to different chemical compositions. While a simple BTAC conditioner could restore some of the hydrophobic domains by depositing a thin hydrophobic layer on the hair surface, it could not completely repair hydrophilic boundaries. This study demonstrates that QNM is a valuable tool for delineating the ultrafine structure of the hair surface, providing mechanistic understanding how hair care products interact with the hair, allowing us to develop solutions for specific hair damage.

Acknowledgments

The authors would like to acknowledge Solomon Wossene and Kimun Park of Croda Inc. for their support with the hair sample preparations and Yang Liu from Bruker for his technical support in QNM.

Conflict of Interest Statement.
None

References.

1. Birbeck M and Mercer E (1957) The electron microscopy of the human hair follicle. Part 1. Introduction and the hair cortex. J. Biophys. Biochem. Cytol. 3: 203–214.
2. Rogers G (1959) Electron microscopy of wool. J. Ultrastruct. Res. 2: 309–330.
3. Swift J (1968) The electron histochemistry of cystine—containing proteins in thin transverse sections of human hair. J. Roy. Microsc. Soc. 88: 449–460.
4. MacMullen R and Zhang G (2011) Investigation of the Internal Structure of Human Hair with Atomic Force Microscopy. J. Cosmet. Sci. 71:117–131.
5. Blach J, Loughlin W, Watson G, Myhra S (2001) Surface characterization of human hair by atomic force microscopy in the imaging and F-d modes. Int. J. Cosmet. Sci. 23: 165-174.
6. Feughelman M, Willis BK (2001) Mechanical extension of human hair and the movement of the cuticle. J. Cosmet. Sci. 52: 185–193.
7. Bhushan B and Chen N (2006) AFM studies of environmental effects on nanomechanical properties and cellular structure of human hair. Ultramicroscopy 106: 755–764.
8. Parbhu A, Bryson W, and Lal R (1999) Disulfide bonds in the outer layer of keratin fibers confer higher mechanical rigidity: correlative nano-indentation and elasticity measurement with an AFM, Biochem. 38: 11755–11761 (1999).
9. Seshadri I and Bhushan B (2008) Effect of rubbing load on nanoscale charging characteristics of human hair characterized by AFM based Kelvin probe. J. Colloid Interface Sci. 325: 580–587.
10. Smith JR, Swift J (2002) Lamellar subcomponent of the cuticular cell membrane complex of mammalian keratin fibres show friction and hardness contrast by AFM. J of Microscopy 206:182–193.
11. Smith J and Swift J (2005) Maple syrup urine disease hair reveals the importance of 18-methyleicosanoic acid in cuticular delamination. Micron 36: 261–266.

12. Sadaie M, Nishikawa M, Ohnishi S, et al (2006) Studies of human hair by friction force microscopy with the hair-model-probe, Colloids Surf. B Biointerfaces, 51:120–129.

13. Pritchard RH, Huang YY, Terentjev EM (2014) Mechanics of biological networks: From the cell cytoskeleton to connective tissue. Soft Matter 10:1864–1884.

14. Picu RC (2011) Mechanics of random fiber networks-a review. Soft Matter 7: 6768–6785.

15. Latorre C, Bhushan B (2005) Nanotribological characterization of human hair and skin using AFM. Ultramicroscopy 105:155-175.

16. Bornschlögla T, Bildsteina L, Thibauta S, et al (2016) Keratin network modifications lead to the mechanical stiffening of the hair follicle fiber. PNAS. 113: 5941-5945.

17. Sedin DL and Rowlen KL (2000) Adhesion forces measured by atomic force microscopy in humid air. Anal. Chem. 72: 2183-2189.

18. Pietak A, Korte S, Tan E, et al (2007) Atomic force microscopy characterization of the surface. Appl. Sur. Sci. 253: 3627–3635.

19. Robbins CR (2009), The cell membrane complex: Three related but different cellular cohesion components of mammalian hair fibers. J. Cosmet. Sci. 60, 437–465.

20. Jones LN, Rivett DE (1997) The role of 18-methyleicosanoic acid in the structure and formation of mammalian hair fibres. Micron 28:469-485.